

THE REVIEW OF PHYSICAL CHEMISTRY OF JAPAN, VOL. 30, No. 2, 1960

THE STRENGTH OF SINGLE CRYSTALS OF INORGANIC SALTS  
UNDER HIGH PRESSURE, IV

BY KAZUO INOUE

(Received November 30, 1960)

On the optical windows for the pressure proof chamber of three kinds of alkali halide single crystals the projections to the atmospheric side of the window were measured, and some considerations were described. Also, using Taylor's equation, the values of  $L$  for the optical windows of sodium chloride, potassium bromide and lithium fluoride were calculated.

For the measurements of the optical properties under high pressure, glass, quartz and alkali halide single crystals are used as the optical windows for pressure proof chambers, and their usable pressure ranges were reported<sup>1-3)</sup>. In Part I of this series<sup>2)</sup>, the bursting process of the optical windows of alkali halide single crystals: sodium chloride, potassium chloride and lithium fluoride under high pressure were observed.

In general, the one surface of the optical window is exposed to high pressure and the other surface to atmospheric pressure. Then the windows subject large shear stress along the peripheral line of the window hole throughout to atmospheric pressure, and then the windows project into the hole. The allowable projection for using as an optical window is divided by the purpose, and no observation is found in regard to the quantitative treatment between the pressure and the plastic deformation into the hole. In the present paper, the heights of the projection due to the pressure on three kinds of alkali halide single crystals were measured, and the experimental equation was found for the second stage of the deformation. Also, using Taylor's equation discussed in Part III<sup>4)</sup>, the distance over which a dislocation could be propagated in the crystal was calculated.

## Experimentals

**Materials** The single crystals used in this experiment, sodium chloride, potassium bromide and lithium fluoride, were made in our laboratory<sup>5)</sup>, and the same as used in Part II<sup>6)</sup>. The shape of specimen is cylindrical or octagonal, 5~15 mm in thickness and 12~28 mm in diameter or in opposite distance, and the both surfaces parallel to the plane of the cleavage were polished as optical plane.

---

1) R. Kiyama, *This Journal*, **19**, 17 (1945)2) R. Kiyama and K. Inoue, *ibid.*, **21**, 78 (1951)3) R. W. Parsons and H. G. Drickamer, *J. Opt. Soc. Am.*, **46**, 464 (1956)4) K. Inoue, *This Journal*, **30**, 80 (1960)5) R. Kiyama and S. Minomura, *ibid.*, **23**, 10 (1953)6) K. Inoue, *ibid.*, **27**, 54 (1957)

**Apparatus and procedure** The apparatus used is the same intensifier as in Part I, and a height finder was fitted to measure the height of the plastic deformation into the hole as shown in Fig. 1. The height of projection of the specimen (S) stuck on the plug (P) was measured with

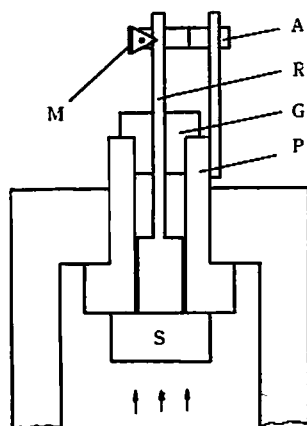


Fig. 1 Experimental apparatus

the displacement of the rod (R), which is vertically movable along the hole and the sleeve (G). The displacements of the rod were measured with the optical lever consisted of the mirror (M) and the arm (A) fixed on the plug. The magnifying power of the optical lever was about 10000 times, and was calibrated with a dial gauge. The pressure was applied with silicone oil, and measured by a Bourdon type pressure gauge. The rate of loading was  $20 \text{ kg/cm}^2$  per minute in all measurements.

## Results

The measured heights of the projection  $h$  at the center in the window hole for various pressures  $p$  were shown in Tables 1~3. The  $h \sim p$  curves obtained from these data showed the parabola in the low pressure range, but in the crystal which has large ratio of the hole diameter to the thickness, the increasing rate of  $h$  decreases temporarily in the pressure range above a certain value. This phenomenon may be understood from the fact that the hydrostatic pressure on the side surface of the crystal becomes effective for the resistance to the flow under high pressure as shown in Fig. 2 (a), and when the ratio is small, as shown in Fig. 2 (b), the crystal is treated as a thin plate, and the shear stress along the periphery of the window hole is the most important factor of the plastic deformation.

In Fig. 3 is shown the atmospheric side of the sodium chloride window, 18mm in hole diameter and 9.5mm in thickness, compressed with the pressure up to  $480 \text{ kg/cm}^2$ . The figure shows many cracks along the (100) and (110) planes and a few cracks along the (111) plane. Similarly, in Fig. 4 is shown the lithium fluoride window, 6.5mm in thickness, blown out by the pressure up to  $700 \text{ kg/cm}^2$ .

Table 1  $h$  values of NaCl ( $10^{-4}$ cm)

Crystal No.	202	203	204	403	404	405	1804	1805
Hole dia., mm	2			4			18	
Thickness, mm	5.6	5.6	5.4	5.2	6.0	5.3	10.2	5.5
Pressure, $p$ kg/cm <sup>2</sup>								
20				—	1.5	1.6	0.7	2.0
40	2.8	3.4	2.4	—	5.3	4.4	1.4	4.7
60				5.9	10.3	8.8	2.1	7.5
80	8.6	9.3	7.7	8.6	14.8	12.6	7.6	10.9
100				11.0	20.2	16.9	14.5	66.1
120	14.1	15.1	13.9	13.1	23.7	20.4	25.2	172
140				16.3	27.2	22.8	38.0	304
160	19.6	20.6	20.9	21.4	28.6	28.5	56.7	457
180				26.6	30.8	32.1	78.1	900
200	24.8	26.3	26.1	—	33.3	35.7	103	
220				38.7	—	38.9	128	
240	29.6	30.9	32.1	40.5	36.2	42.1	156	
260				42.1	38.0	44.9	191	
280	35.6	36.3	37.7	45.6	40.4	48.3	226	
300				49.2	42.9	51.3	264	
320	41.4	41.5	44.0	52.6	45.4		302	
340				56.1	46.8			
360	48.7	43.9	49.2	60.3	47.9			
380				—	48.6			
400	58.0	45.3	55.2	69.4	50.3			
420				72.9	53.4			
440	65.7	46.0	61.7	77.1	55.3			
460				79.9	57.5			
480	72.0	46.8	66.8	82.7	61.0			
500	74.8	47.8	69.7	87.5	63.9			
550	78.7	49.4	73.6					
600	83.2	51.5	75.7					
650	85.3	53.3	77.4					
700	87.4	55.8	79.6					
750	90.2	58.4	81.7					
800	95.9	61.9	83.2					

In the specimen subjected to large deformation, as shown in Fig. 5, it was found that the surface of the high pressure side of the window caved in the shape of square along the (110) plane, and this phenomenon observed the most clearly in potassium bromide.

### Considerations

As shown in the schematic diagrams in Part I, the forms of the projection in the window hole change through various processes to reach the breakdown. It may be treated quantitatively only under the condition B in Fig. 2 of Part I, and thus the variation was shown more precisely in Fig. 6. There are three stages, the first stage (a), which follows Hooke's law called the elastic range, the second stage (b), in which the spherical plastic deformation appears along the periphery of the window hole, and radius of curvature of the sphere changes with increasing pressure, and the third stage (c), in which after the radius of curvature reaches a certain value, the extrusion

Table 2  $h$  values of KBr ( $10^{-4}$ cm)

Crystal No.	201	401	1802
Hole dia, mm	2	4	18
Thickness, mm	4.7	4.8	11.6
Pressure, $p$ kg/cm <sup>2</sup>			
40	3.1	3.8	2.0
80	7.2	8.9	26.8
120	12.3	15.5	90.8
160	17.6	25.9	195
200	23.7	38.5	331
240	31.9	53.2	484
280	40.5	70.3	694
320	49.6	90.5	
360	59.6	114	
400	68.5	139	
440	77.5		
480	87.2		
500	92.5		
550	105		
600	115		

Table 3  $h$  values of LiF ( $10^{-4}$ cm)

Crystal No.	1801	1802
Hole dia, mm	18	
Thickness, mm	6.4	6.3
Pressure, $p$ kg/cm <sup>2</sup>		
50	0.7	1.6
100	2.1	4.3
150	5.5	9.3
200	11.7	25.5
250	29.9	93.7
300	117	206
350	202	309
400	286	409
450	377	539
500	486	651
550	603	808
600	696	
650	835	

occurs in the whole surface of the hole. The pressure which shifts from a stage to the next stage, is decided with the kind of crystal, the hole diameter and the thickness.

From the values in Tables 1~3, the relations between  $\log h$  and  $\log p$  were classified according to the above three stages shown as an example in Fig. 7. In the first stage, the inclination of the curve differed with the ratio of the hole diameter to the thickness, but in this range, the amount of deformation is very small, and moreover the measured points are poor, nothing can be said in this range. In the second stage,  $\log h$  is proportional to  $\log p$  in all crystals; hence the following relation is given for this stage.

$$h = Cp^A.$$

The parameter  $A$  is a function of the kind of crystal, the hole diameter and the thickness of the crystal. The values of  $A$  from the experiments were shown in Table 4 with the pressure range of the second stage in each crystal. In the third stage, the extrusion in the whole surface of the hole is attended with the cracks as above mentioned, and the projection height seems not proportional to the pressure. This range can be treated only for the crystals able to elongate largely as metals.

In spite of the values of  $A$  for the second stage shown in Table 4, since the pressure range of the stage is narrow, the author attempted to make the application of Taylor's equation, in which it was assumed that the shear is proportional to square of the shear stress, only for the second stage of crystals for 18mm in hole diameter. As mentioned in Part III, the following equation is given by Taylor<sup>7)</sup> on the relation between the shear strain  $\gamma$  and the shear stress  $f$ ,

7) G. I. Taylor, *Proc. Roy. Soc. (London)*, **A145**, 362, 388, 405 (1934)

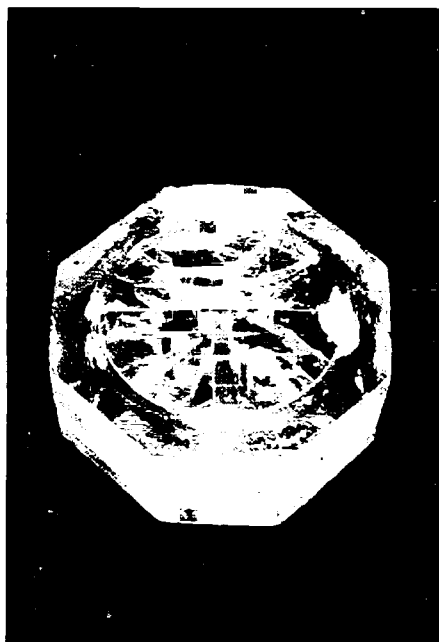


Fig. 3 Photograph of the cracked specimen  
crystal: NaCl  
hole diameter: 18 mm  
thickness: 9.5 mm  
max. pressure: 480 kg/cm<sup>2</sup>



Fig. 4 Photograph of the crushed specimen  
crystal: LiF  
hole diameter: 18 mm  
thickness: 6.5 mm  
crushed pressure: 700 kg/cm<sup>2</sup>

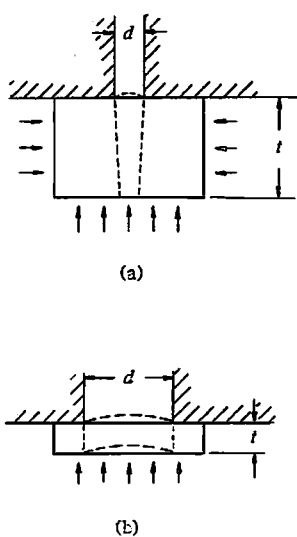


Fig. 2 Effect of pressure on the side surface of the window

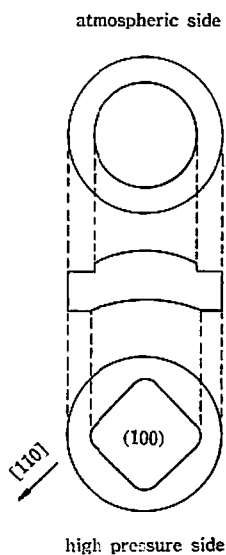


Fig. 5 Schematic diagram of the cavity appeared on the high pressure side of the specimen

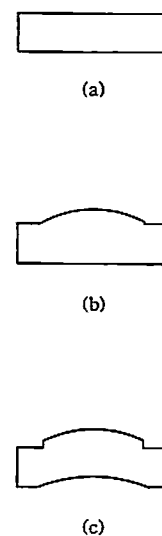
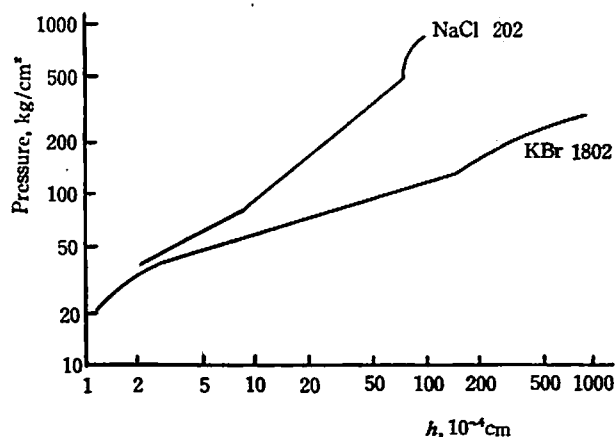


Fig. 6 Schematic diagrams of three stages before cracking with pressure

Fig. 7 Examples of  $\log h \sim \log p$  curvesTable 4 The pressure range of the second stage and  $A$  values

Crystal	Hole dia. mm	Thickness mm	Pressure range kg/cm <sup>2</sup>	$A$
NaCl 202	2	5.6	80-480	1.09
NaCl 203	"	5.6	80-320	1.09
NaCl 204	"	5.4	80-480	1.09
KBr 201	2	4.7	80-200	1.57
NaCl 403	4	5.2	60-140	1.23
NaCl 404	"	6.0	40-100	1.46
NaCl 405	"	5.3	40-150	1.40
KBr 401	4	4.8	20-100	1.80
NaCl 1804	4	10.2	60-120	3.04
NaCl 1805	"	5.5	60-100	8.64
KBr 1802	18	11.6	40-100	3.73
LiF 1801	18	6.4	200-350	5.79
LiF 1802	"	6.3	170-310	5.79

$$\gamma = \frac{L}{C^2 G^2 \lambda} f^2, \quad (1)$$

where  $G$  is the modulus of shear,  $\lambda$  the interval of the atoms in the direction of gliding,  $C$  a constant depending on the particular arrangement of the center of dislocation, which is said to be 0.17 for square lattice of dislocation, and  $L$  the mean free path of the dislocation.

The crystal for 18 mm in hole diameter is considered as a thin plate, then the shear stress  $f$  is given by the following equation,

$$f = \frac{dp}{4t}, \quad (2)$$

and the shear strain  $\gamma$  is nearly equal to  $\tan \gamma$ , when  $\gamma$  has small value, then

$$\gamma \approx \tan \gamma = \frac{4hd}{d^2 - 4h^2} \approx \frac{4h}{d}. \quad (3)$$

Combining Eq. (1) with Eqs. (2) and (3), the resulting equation is

$$L = 64C^2G^2\lambda \frac{l^2}{d^3} \frac{h}{p^2} \quad (4)$$

The calculated values of  $L$  are given in Table 6, using the  $h/p^2$  values in Table 5 from the data in Tables 1~3. These values of  $L$  are smaller than the results of Part III in all crystals, and the conceivable reason of this fact is that the window is treated as the thin plate.

Table 5  $h/p^2$  values in Eq. (4) for the second stage of 18mm in hole diameter

Crystal	$l^2/d^3$	$h$ $10^{-4}$ cm	$p$ kg/cm <sup>2</sup>	$h/p^2$ cm <sup>5</sup> kg <sup>-2</sup>	mean
NaCl 1804	0.178	2.1	60	$5.83 \times 10^{-8}$	$1.24 \times 10^{-7}$
		7.6	80	$1.19 \times 10^{-7}$	
		14.5	100	$1.45 \times 10^{-7}$	
		25.2	120	$1.75 \times 10^{-7}$	
NaCl 1805	0.0519	7.5	60	$2.08 \times 10^{-7}$	$3.46 \times 10^{-7}$
		10.9	80	$1.70 \times 10^{-7}$	
		66.1	100	$6.61 \times 10^{-7}$	
KBr 1802	0.231	2.0	40	$1.25 \times 10^{-7}$	$3.43 \times 10^{-7}$
		9.6	60	$2.67 \times 10^{-7}$	
		26.8	80	$4.19 \times 10^{-7}$	
		55.9	100	$5.59 \times 10^{-7}$	
LiF 1801	0.0702	11.7	200	$2.93 \times 10^{-8}$	$9.28 \times 10^{-8}$
		29.9	250	$4.78 \times 10^{-8}$	
		117	300	$1.30 \times 10^{-7}$	
		202	350	$1.64 \times 10^{-7}$	
LiF 1802	0.0681	25.5	200	$6.38 \times 10^{-8}$	$1.48 \times 10^{-7}$
		93.7	250	$1.50 \times 10^{-7}$	
		206	300	$2.29 \times 10^{-7}$	

Table 6  $L$  values for the second stage of 18mm in hole diameter

Crystal	$\lambda$ $10^{-8}$ cm	$G$ $10^8$ kg/cm <sup>2</sup>	$h/p^2$ cm <sup>5</sup> kg <sup>-2</sup>	$L$ cm
NaCl	3.98	1.847	$1.24 \times 10^{-7}$	$5.32 \times 10^{-8}$
			$3.46 \times 10^{-7}$	$4.33 \times 10^{-8}$
KBr	4.66	1.485	$3.43 \times 10^{-7}$	$1.46 \times 10^{-4}$
LiF	2.84	2.908	$9.28 \times 10^{-8}$	$2.73 \times 10^{-8}$
			$1.48 \times 10^{-7}$	$4.32 \times 10^{-8}$

The author has great pleasure in expressing his sincere thanks to Prof. Wasaburo Jono for his valuable guidance and encouragement throughout the course of this investigation. He is also grateful to Prof. Eiji Suito and Dr. Natsu Ueda for their kind discussion in the present investigation.

*The Laboratory of Physical Chemistry  
Kyoto University  
Kyoto, Japan*